PCCP

RSC Publishing

PAPER

View Article Online
View Journal | View Issue

Comparison of MM/GBSA calculations based on explicit and implicit solvent simulations

Cite this: *Phys. Chem. Chem. Phys.*, 2013, **15**, 7731

Frithjof Godschalk, Samuel Genheden, Pär Söderhjelm and Ulf Ryde*

Molecular mechanics with generalised Born and surface area solvation (MM/GBSA) is a popular method to calculate the free energy of the binding of ligands to proteins. It involves molecular dynamics (MD) simulations with an explicit solvent of the protein–ligand complex to give a set of snapshots for which energies are calculated with an implicit solvent. This change in the solvation method (explicit → implicit) would strictly require that the energies are reweighted with the implicit-solvent energies, which is normally not done. In this paper we calculate MM/GBSA energies with two generalised Born models for snapshots generated by the same methods or by explicit-solvent simulations for five synthetic *N*-acetyllactosamine derivatives binding to galectin-3. We show that the resulting energies are very different both in absolute and relative terms, showing that the change in the solvent model is far from innocent and that standard MM/GBSA is not a consistent method. The ensembles generated with the various solvent models are quite different with root-mean-square deviations of 1.2–1.4 Å. The ensembles can be converted to each other by performing short MD simulations with the new method, but the convergence is slow, showing mean absolute differences in the calculated energies of 6–7 kJ mol^{-1} after 2 ps simulations. Minimisations show even slower convergence and there are strong indications that the energies obtained from minimised structures are different from those obtained by MD.

Received 10th January 2013,
Accepted 2nd April 2013

DOI: 10.1039/c3cp00116d

www.rsc.org/pccp

Introduction

Molecular mechanics with generalised Born and surface-area solvation (MM/GBSA)[1,2] is among the most popular methods to estimate protein–ligand binding affinities,[3,4] to find important residues for protein–protein interactions,[5,6] and to study macromolecular stability.[1,7] When computing the MM/GBSA free energy, the system of interest is first simulated using either molecular dynamics (MD) or Metropolis Monte Carlo and snapshots are sampled at regular intervals. Second, for each snapshot, the following free energy is calculated in a post-processing step

$$G = E_{\mathrm{int}} + E_{\mathrm{ele}} + E_{\mathrm{vdw}} + G_{\mathrm{pol}} + G_{\mathrm{np}} - TS \qquad (1)$$

where the first three terms on the right-hand side are the molecular-mechanics internal, electrostatic, and van der Waals energies, respectively. G_{pol} and G_{np} are the polar and non-polar solvation free energies, and T and S are the absolute temperature and an entropy estimate, respectively. Usually, the system is solvated in a box of explicit water molecules during the simulation. These solvent molecules are removed before the post-processing and replaced with an implicit representation, using either the generalised Born (GB) or Poisson–Boltzmann methods together with a surface-area term (the G_{pol} and G_{np} terms in eqn (1)).[4,8] Thus, the solvent model and therefore the Hamiltonian are different in the simulation and in the post-processing, an inconsistency that has hardly been discussed.

Strictly, such a shift in the Hamiltonian requires that the snapshots should be reweighted with the new (implicit-solvent) energy function. When computing the average MM/GBSA energy over all snapshots, each snapshot should be assigned a weight that is the Boltzmann factor of the difference between the energies with the simulation Hamiltonian (explicit solvent) and the post-processing Hamiltonian (implicit solvent). However, this is normally ignored and a plain average is computed, *i.e.*, all snapshots are weighted equally.

An alternative is to perform also the simulation in implicit solvent, thereby circumventing the reweighting and giving a solvent-consistent MM/GBSA method. However, an implicit solvent is a theoretically less rigorous approach than explicit solvent, and it is not certain that the two sampling approaches will give equivalent ensembles.[9] In addition, implicit-solvent simulations sometimes give poor results, *e.g.* dissociation of ligands or protein subunits.[10]

Department of Theoretical Chemistry, Lund University, Chemical Centre, P. O. Box 124, SE-221 00 Lund, Sweden. E-mail: Ulf.Ryde@teokem.lu.se; Fax: +46 46 2228648; Tel: +46 46 2224502

In this paper, we make a thorough comparison of MM/GBSA energies calculated from simulations with either implicit or explicit simulations. Furthermore, we quantify the similarity of the obtained snapshots by converting the explicit solvent-simulated snapshots to implicit simulated-snapshots using short MD simulations or minimisations. As a test case, we use the binding of five inhibitors to the carbohydrate-recognition domain of the protein galectin-3 (gal3). These systems have been used previously in MM/GBSA calculations[11] and they have also been studied experimentally.[12]

Methods

System preparation

The five ligands illustrated in Fig. 1 were studied when bound to gal3. The five ligands are synthetic *N*-acetyllactosamine derivatives and will be denoted as in the original publication,[12] *viz.*, **2** through **6**. The crystal structures of the complexes of gal3 with ligands **2** and **3** (PDB codes: 2XG3[13] and 1KJR[12]) were used as starting structures for the simulation of these ligands. For ligands **4**, **5**, and **6**, we used the crystal structure of gal3–**3** after removing the methoxy group of **3** and replacing fluorine with hydrogen atoms. This structure was used because ligands **4**, **5**, and **6** are all fluorinated and therefore expected to have a binding mode similar to that of **3**, whereas **2** is not fluorinated and displays a different binding mode regarding the conformation of Arg-144, as can be seen in Fig. 2. The preparation of the protein has been described in detail previously.[11] All residues were assigned their normal protonation states at pH 7, *i.e.* all Asp and Glu residues were negatively charged and all Lys and Arg residues were positively charged. The His residue at the binding site (His-158) was protonated on the ND1 atom, whereas the other three His residues were protonated on the NE2 atom. The protein was described with the Amber99SB force field[14] and the ligands were described with the general Amber force field.[15] Charges for the ligands were obtained by restrained electrostatic potential (RESP) calculations[16] on ESPs calculated at the Hartree–Fock/6-31G* level and sampled with the Merz–Kollman scheme.[17]

Implicit simulations

All MD simulations were run by the *sander* module of Amber11. Two implicit solvation models were tested, *viz.* the generalised Born models by Mongan *et al.* (GBn)[18] and by Onufriev, Bashford, and Case (GB^{OBCI}; the first model, *i.e.* with the three parameters set to 0.8, 0.0, and 2.9).[19] For GBn, Bondi radii[20] were used, whereas the second set of modified Bondi radii (mbondi2)[19] was used with GB^{OBCI}. The non-polar solvation was calculated by multiplying the solvent-accessible surface-area (SA) with a surface-tension parameter, *i.e.*, γSA.[21] SA was estimated by the LCPO method[22] (linear combinations of pairwise overlaps) and γ was set to 0.021 kJ mol^{-1} Å^{-2}. The non-bonded cutoff, as well as the cutoff for the calculation of the effective Born radius, were set to 15 Å. The temperature was kept at 300 K using Langevin dynamics[23] with a collision frequency of 2 ps^{-1}. All bonds to hydrogen atoms were constrained using SHAKE[24] and a 2 fs time step was used for the integration of motion. The forces of slowly-varying motions (the derivatives with respect to effective Born radii and pair interactions whose distances are greater than 8 Å) were evaluated every second step, and the non-bonded pair list was updated every 25 steps.

The protein–ligand complexes were first minimised by 500 steps of steepest descent, using a harmonic restraint towards the crystal structure with a force constant of 418.4 kJ mol^{-1} Å^{-2} on non-hydrogen atoms, followed by a 20 ps MD simulation with the same restraints but with the force constant halved, and a 1000 ps MD simulation without any restraints. The final structure of this simulation was used to start 40 independent simulations by assigning different initial velocities. Each independent simulation was further simulated for 300 ps, and snapshots were extracted every 5 ps during the last 200 ps. This has shown to be a proper simulation protocol for gal3.[11]

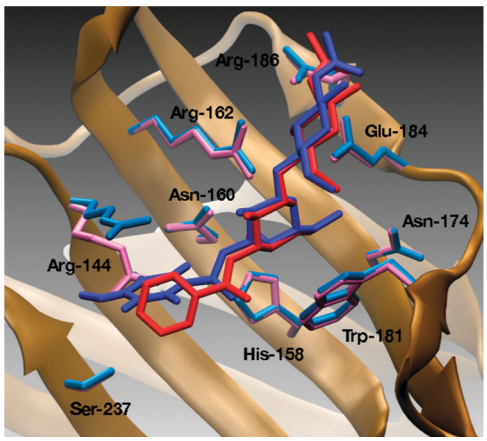

Fig. 2 Overlay of the crystal structures of gal3 in complex with **2** (PDB id 2XG3[13]) in red and in complex with **3** (PDB id 1KJR[12]) in blue. The closest residues are shown in light red and light blue, respectively, with the only significant deviation seen for Arg-144, which forms a stacking interaction on opposite faces of the aromatic ring of the ligand.

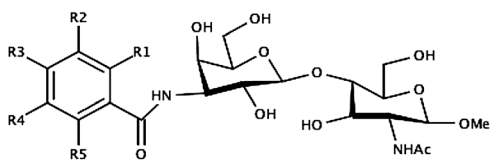

Ligand	R1	R2	R3	R4	R5
2	H	H	H	H	H
3	F	F	OMe	F	F
4	F	F	F	F	F
5	H	F	F	F	F
6	H	F	H	F	H

Fig. 1 The five ligands investigated in this study. The numbering of the ligands follows the original study.[12]

Explicit simulations

The systems were solvated in a pre-equilibrated truncated octahedral box of TIP4PEw water molecules.[25] The temperature was kept at 300 K using Langevin dynamics[23] as for the implicit simulations, and the pressure was kept at 1 atm using an isotropic weak-coupling algorithm[26] with a relaxation time of 1 ps. SHAKE[24] was used to constrain bonds to hydrogen atoms and the time step was 2 fs. The cut-off for the van der Waals interactions was 8 Å and the long-range correction was estimated using a continuum approach.[27] Electrostatic interactions were computed using particle-mesh Ewald summation[28] with a fourth-order B-spline interpolation, a tolerance of 10^{-5} and a real-space cut-off equal to 8 Å. The non-bonded pair list was updated every 25 step. The simulation protocol, *i.e.*, the minimisation, equilibration, and production MD simulations, was identical to that used for the implicit simulations.

MM/GBSA calculations

The binding free energy between the protein and a ligand was estimated by

$$\Delta G = \langle G(\mathrm{PL}) - G(\mathrm{P}) - G(\mathrm{L})\rangle_{\mathrm{PL}} \quad (2)$$

where PL, P, and L are the protein–ligand complex, the protein, and the ligand, respectively, and the free energy of each of these species was calculated using eqn (1).[1] The brackets indicate an average over snapshots from the MD simulations of the complex. To compute the energies for the protein and the ligand, the coordinates of the other moiety were removed. This is the standard approach of MM/GBSA, giving precise energies in an efficient manner.[29] Moreover, the E_{int} term in eqn (1) cancels out.

The E_{int}, E_{ele}, and E_{vdw} terms in eqn (1) were evaluated using the same force field as in the simulation, but without any cutoff. The G_{pol} and G_{np} terms were estimated using the same methods used in the implicit simulation, *i.e.* with GBn or $\mathrm{GB}^{\mathrm{OBCI}}$ and γSA. The entropy was calculated as a combination of the rotational and translational entropy from standard formulas for gas-phase molecules and the vibrational entropy, calculated from frequencies obtained by a normal-mode analysis. The normal-mode analysis was computed on truncated systems as described previously[30] yielding an improved precision and efficiency.[31] For each protein–ligand complex and solvation model, we calculated the MM/GBSA energy on 40 snapshots from 40 independent simulations, *i.e.*, 1600 snapshots in total.

Statistical analysis

Each reported uncertainty of MM/GBSA estimates is the standard deviation of the mean over the 40 independent simulations, *i.e.*, the standard deviation over the average MM/GBSA result from the 40 independent simulations divided by $\sqrt{40}$. The MM/GBSA estimates were compared to experimental free energies using the mean unsigned error after removal of the systematic error (*i.e.* the mean signed deviation from the experimental results; MUEtr), the correlation coefficient (r^2), and Kendall's rank correlation coefficient (τ). The uncertainties of these quantities were obtained by a bootstrapping procedure outlined previously.[11]

Results and discussion

We have estimated binding affinities of five ligands to gal3 using MM/GBSA. The MM/GBSA calculations were based on snapshots generated using MD simulation with either explicit TIP4PEw water molecules or two implicit GB methods. In what follows, we will discuss the binding affinities obtained and the differences between the snapshots generated with the different solvent models.

Binding affinities

The computed binding affinities are shown in Table 1 for the various combinations of solvent models used in the MD simulations and energy post-processing. In the conventional MM/GBSA approach, the protein–ligand complex is simulated with an explicit solvent representation.[4] Using such an approach and post-processing the snapshots with the GBn model gives binding affinities that are anti-correlated with the experimental binding affinities. The correlation coefficient (r^2) is 0.78 ± 0.06, but Kendall's τ of −0.78 ± 0.04 shows that a majority of the affinities are incorrectly ranked. The mean unsigned error after removal of the systematic error (MUEtr)

Table 1 MM/GBSA estimates of the binding free energy (kJ mol^{-1}), using different combinations of solvent models in the MD simulations and the energy evaluations

Energy[a]	GBn			$\mathrm{GB}^{\mathrm{OBCI}}$			
MD[b]	GBn	$\mathrm{GB}^{\mathrm{OBCI}}$	TIP4PEw	GBn	$\mathrm{GB}^{\mathrm{OBCI}}$	TIP4PEw	Exp
2	−169.2 ± 2.4	−6.5 ± 2.8	−76.1 ± 3.8	−93.6 ± 0.5	−87.2 ± 0.7	−75.8 ± 1.1	−29.7
3	−182.3 ± 1.9	−39.7 ± 3.9	−66.6 ± 3.0	−95.5 ± 0.6	−87.1 ± 0.7	−89.6 ± 0.8	−34.8
4	−156.1 ± 2.2	−52.7 ± 1.8	−107.1 ± 2.4	−89.9 ± 0.4	−75.1 ± 0.5	−91.2 ± 0.6	−24.5
5	−131.4 ± 3.4	−35.3 ± 2.2	−86.8 ± 4.6	−89.4 ± 0.6	−86.5 ± 0.7	−98.7 ± 1.4	−29.7
6	−178.0 ± 2.2	−68.6 ± 2.5	−120.2 ± 3.9	−83.0 ± 0.6	−81.3 ± 0.7	−101.0 ± 0.8	−26.3
MUEtr	14.2 ± 1.2	19.0 ± 1.1	20.7 ± 1.5	2.7 ± 0.2	2.4 ± 0.3	9.4 ± 0.4	
$r^{2\,c}$	0.07 ± 0.03	−0.20 ± 0.06	−0.78 ± 0.06	0.50 ± 0.05	0.70 ± 0.06	−0.07 ± 0.02	
τ	0.33 ± 0.06	−0.33 ± 0.08	−0.78 ± 0.04	0.56 ± 0.10	0.78 ± 0.17	−0.33 ± 0.08	
Range	50.9	62.0	53.6	12.5	12.2	25.3	10.3

[a] The solvent model used in the MM/GBSA energy post-processing. [b] The solvent model used in the MD simulations to generate the snapshots. [c] A negative sign or r^2 indicates that r is negative.

is 21 ± 2 kJ mol^{-1}, which is much larger than for the null hypothesis that all ligands have the same affinity (MUEtr = 2.9 kJ mol^{-1}). This is mostly caused by the exaggerated range of the MM/GBSA estimates, 54 kJ mol^{-1} compared to 10 kJ mol^{-1} for the experimental affinities, which leads to a slope that is much larger than 1.

If we instead use the GB^{OBCI} method for the G_{pol} term on the same snapshots, the results are not improved. The correlation coefficient is basically zero, τ shows that most of the affinities are incorrectly ranked, and the MUEtr of 9.4 ± 0.4 kJ mol^{-1} is larger than for the null hypothesis. However, the difference in uncertainty of the two approaches is interesting. GBn gives consistently a worse precision than GB^{OBCI}, 3.5 kJ mol^{-1} compared to 0.9 kJ mol^{-1} on average. From Table 2, it can be seen that this comes entirely from the G_{pol} term, which has an average precision of 3.3 kJ mol^{-1} when evaluated with the GBn model but 1.1 kJ mol^{-1} when evaluated with the GB^{OBCI} model. The second largest uncertainty is for the electrostatic term, 1.5 kJ mol^{-1} on average for both models. The other terms have uncertainties that are smaller than 1 kJ mol^{-1}. Hence, the uncertainty of the GBn estimates is dominated by the uncertainty in the G_{pol} term, whereas the uncertainty of the GB^{OBCI} estimates is dominated by the E_{ele} term.

An alternative to simulate with explicit water is to simulate with the same GBSA model used in the energy post-processing, an approach we will call solvent-consistent MM/GBSA (sc-MM/GBSA) in the following. Such binding affinities have been estimated as well, and using GBn both in the simulations and the energy calculations improves the affinities compared to the explicit-solvent simulation. However, the results are still quite poor, with basically no correlation and a MUEtr (14 ± 1 kJ mol^{-1}) that is much larger than for the null hypothesis.

However, if we instead use the GB^{OBCI} model both in the MD simulations and the energy calculations, we obtain good affinities. The correlation coefficient is decent (r^2 = 0.70 ± 0.06) and the τ of 0.8 ± 0.2 shows that most of the affinities are correctly ranked. Moreover, MUEtr (2.4 ± 0.3 kJ mol^{-1}) is lower than for the null hypothesis, showing that the affinities are good on a relative scale, although the estimation is much more negative than the experimental affinities (by 61 kJ mol^{-1} on average). A similar remarkable difference in MM/GBSA binding affinities obtained with the two GB models has previously been observed for the avidin protein.[9] Again, there is also a large difference in the precision of the binding affinities obtained with the two approaches. The average precision when using the GBn model is 2.4 kJ mol^{-1}, whereas the corresponding value for the GB^{OBCI} model is only 0.7 kJ mol^{-1} (see Table 2). It is noteworthy that these uncertainties are smaller than when the simulation was performed with explicit solvent, indicating that there is some mismatch between the ensembles generated with explicit and implicit solvent.

It is also interesting to estimate affinities from energies calculated by one GB model and based on simulation with the other GB model. These estimates are shown in Table 1 as well. Using the GBn model to post-process snapshots generated with the GB^{OBCI} model gives poor results: there is a negative correlation and most of the affinities are incorrectly ranked, as is indicated by τ = −0.3 ± 0.1. The range of the estimates is about six times as large as the range of the experimental affinities, leading to a MUEtr that is much worse than the MUEtr of the null hypothesis (19 ± 1 kJ mol^{-1}). However, if we instead use the GB^{OBCI} model to post-process snapshots generated with the GBn model, we obtain quite good results: r^2 = 0.50 ± 0.05 and τ = 0.6 ± 0.1, whereas MUEtr = 2.7 ± 0.2 kJ mol^{-1} is on par with the null hypothesis. These results indicate that the GBn method gives reasonable structures but unstable energies, which is also corroborated by the larger uncertainties of the GBn energies in Tables 1 and 2.

In Table 3, we list the term-wise difference between sc-MM/GBSA estimates obtained with the GBn and GB^{OBCI} models. It is clear that the largest difference comes from the G_{pol} term, between −39 and −101 kJ mol^{-1}, and −74 kJ mol^{-1} on average. There are smaller differences also for the other terms and the differences are for most of the ligands statistically significant. Besides G_{pol}, the E_{ele} term shows the largest variation among the ligands, with differences between −30 and 2 kJ mol^{-1}. Of course, this difference is caused by differences in the structures generated by the two methods (for the same snapshot, the two methods differ only in the G_{pol} term). The G_{np} term shows the smallest variation among ligands and also the smallest difference between the two sc-MM/GBSA approaches. It is also the term that makes the smallest contribution to the free energy.

Moreover, we have compared the MM/GBSA terms obtained with the GB^{OBCI} model for snapshots generated either with GB^{OBCI} or TIP4PEw solvation. From Table 3B, it can be seen that the difference in the G_{pol} term is smaller (because the energies are calculated with the same GB^{OBCI} model) and that the differences in the E_{ele} and G_{pol} terms to a large degree cancel out, so that it is actually the E_{vdw} term that dominates for all ligands except **2**.

Table 2 Average uncertainty over the five ligands (kJ mol^{-1}) for the various terms of different combinations of solvent models in the MD simulation and the energy evaluation

Energy model	GBn			GB^{OBCI}		
MD model	GBn	GB^{OBCI}	TIP4PEw	GBn	GB^{OBCI}	TIP4PEw
E_{ele}	0.8	1.5	1.5	0.8	1.5	1.5
E_{vdw}	0.5	0.4	0.7	0.5	0.4	0.7
G_{pol}	2.5	2.7	3.3	0.7	1.1	1.1
G_{np}	0.0	0.0	0.1	0.0	0.0	0.1
$-TS$	0.4	0.6	0.7	0.4	0.6	0.7
ΔG	2.4	2.6	3.5	0.6	0.7	0.9

RMSD analysis

It is of interest to quantify also the geometric differences between the three generated ensembles. We started by computing the root mean square deviation (RMSD) between the various snapshots and the crystal structure for the heavy atoms of the protein backbone. The results are shown in Table 4. It is clear that the explicit-solvent model gives snapshots that are closest to the crystal structure. The RMSD is ∼0.7 Å for all ligands. With the GBn model, we obtain slightly larger RMSDs, between

Table 3 Term-wise differences in kJ mol^{-1} (A) between sc-MM/GBSA estimates using GBn and GB^{OBCI}, and (B) between the MM/GBSA estimates (obtained with GB^{OBCI} for the energy calculation) using GB^{OBCI} and TIP4PEw trajectories

	A					B				
Ligand	E_{ele}	E_{vdw}	G_{pol}	G_{np}	$-TS$	E_{ele}	E_{vdw}	G_{pol}	G_{np}	$-TS$
2	2.2	7.6	−87.5	0.3	−4.7	−15.0	−7.4	3.8	−1.1	8.2
3	−18.7	7.5	−87.7	0.4	3.2	18.3	8.4	−17.9	0.5	−6.8
4	−30.0	−0.7	−53.2	−0.7	3.6	38.8	11.7	−31.7	1.0	−3.7
5	−15.6	1.5	−39.1	−0.4	8.6	16.4	20.5	−26.2	1.6	−0.1
6	−7.3	5.8	−100.8	0.2	5.3	13.0	19.8	−18.6	1.9	3.7
Average	−13.9	4.3	−73.7	0.0	3.2	14.3	10.6	−18.1	0.8	0.3

A negative difference indicates that the GBn estimate is more negative than the GB^{OBCI} estimate (A) or that the results for the GB^{OBCI} trajectories are more negative than those for the TIP4PEw trajectories (B).

Table 4 Average RMSD from the crystal structure (Å) for protein backbone atoms of the snapshots used in the MM/GBSA estimates

Solvent model	GBn	GB^{OBCI}	TIP4PEw
2	1.11 ± 0.01	1.10 ± 0.01	0.73 ± 0.01
3	1.07 ± 0.01	1.32 ± 0.01	0.79 ± 0.01
4	1.00 ± 0.00	1.48 ± 0.01	0.69 ± 0.00
5	1.14 ± 0.01	1.48 ± 0.01	0.73 ± 0.01
6	1.22 ± 0.02	1.30 ± 0.01	0.72 ± 0.01
Average	1.11	1.34	0.73

1.0 and 1.2 Å (1.1 Å on average), and with the GB^{OBCI} model, we obtain even larger RMSDs of 1.1–1.5 Å (1.3 Å on average). These results follow the expectations, because the explicit TIP4PEw model, which is expected to give the most accurate results, gives trajectories closest to the crystal structure and the more modern GB model (GBn) gives trajectories closer to the crystal structure than the older GB^{OBCI} model. However, it does not explain why the GB^{OBCI} model gave better affinities than the GBn model.

Next, we computed the RMSD between the snapshots in the same ensemble, *i.e.* between snapshots generated with the same solvent model. These measurements are listed in the upper part of Table 5. For the TIP4PEw ensemble, we obtain RMSDs between 0.6 and 0.7 Å for the protein backbone and 1.2–1.3 Å for the ligand. For the GBn ensemble, the variation is slightly larger with an average backbone RMSD of 0.9 Å and an average ligand RMSD of 1.3 Å. The GB^{OBCI} ensemble gives even larger RMSD, 1.0 Å for the backbone and 1.4 Å for the ligand on average. The latter finding is consistent with the larger uncertainties for the GB^{OBCI} snapshots in all MM/GBSA terms except E_{vdw}, as shown in Table 2.

We also computed the RMSD between snapshots from different ensembles, *i.e.* between snapshots generated with different solvent models. These measurements are shown in the lower part of Table 5. Comparing the GBn and TIP4PEw ensembles, we obtain an average RMSD of 1.2 and 1.7 Å for the protein backbone and the ligand, respectively. This is higher than the average RMSDs for the individual GBn and TIP4PEw ensembles, indicating the two ensembles are more different than the snapshots within the ensembles. However, the difference observed for the ligand RMSD is not statistically significant for all ligands. The same observation holds true when comparing the GB^{OBCI} and TIP4PEw ensembles, and when comparing the GB^{OBCI} and the GBn ensembles. However, the RMSD analysis does not indicate that any ensemble is more different than the other, because for most ligands, the differences between the inter-ensemble RSMD measurements are not statistically significant.

Table 5 Average RMSD (in Å) between the various snapshots used in the MM/GBSA estimates. The RMSD was calculated for every possible pair of snapshots taken every 50 ps in the simulations

Solvent model	GBn/GBn		GB^{OBCI}/GB^{OBCI}		TIP4PEw/TIP4PEw	
	Backbone	Ligand	Backbone	Ligand	Backbone	Ligand
2	0.96 ± 0.02	1.34 ± 0.17	1.01 ± 0.04	1.38 ± 0.17	0.67 ± 0.01	1.28 ± 0.37
3	0.97 ± 0.02	1.41 ± 0.23	0.91 ± 0.05	1.47 ± 0.25	0.66 ± 0.01	1.19 ± 0.27
4	0.80 ± 0.05	1.24 ± 0.10	1.18 ± 0.07	1.49 ± 0.27	0.61 ± 0.01	1.19 ± 0.28
5	0.94 ± 0.03	1.27 ± 0.12	1.02 ± 0.04	1.33 ± 0.14	0.67 ± 0.01	1.25 ± 0.34
6	1.00 ± 0.03	1.32 ± 0.15	0.88 ± 0.05	1.34 ± 0.15	0.71 ± 0.01	1.23 ± 0.32
Average	0.93	1.32	1.00	1.40	0.66	1.23
Solvent model	GBn/TIP4PEw		GB^{OBCI}/GBn		GB^{OBCI}/TIP4PEw	
	Backbone	Ligand	Backbone	Ligand	Backbone	Ligand
2	1.14 ± 0.02	1.88 ± 0.56	1.15 ± 0.03	1.40 ± 0.09	1.15 ± 0.04	1.89 ± 0.59
3	1.17 ± 0.04	1.54 ± 0.15	1.25 ± 0.04	1.53 ± 0.17	1.33 ± 0.07	1.70 ± 0.35
4	1.01 ± 0.01	1.50 ± 0.15	1.37 ± 0.08	1.47 ± 0.13	1.59 ± 0.23	1.65 ± 0.29
5	1.21 ± 0.02	1.80 ± 0.21	1.29 ± 0.05	1.45 ± 0.11	1.57 ± 0.22	1.95 ± 0.68
6	1.23 ± 0.02	1.59 ± 0.18	1.10 ± 0.03	1.36 ± 0.07	1.33 ± 0.07	1.68 ± 0.32
Average	1.15	1.66	1.23	1.44	1.39	1.77

Converting explicit-solvent generated snapshots to solvent-consistent snapshots

Owing to the large fluctuations of the total energies, it is not possible to directly reweight the snapshots from the explicit-solvent simulations to the implicit-solvent Hamiltonian. As an alternative, we can attempt to convert the snapshots to the solvent-consistent ensemble using short MD simulations or minimisations. In some implementations of a semiempirical quantum-mechanics variant of MM/GBSA, it is standard to minimise snapshots with the semiempirical Hamiltonian before computing eqn (1),[32,33] and here we attempt something similar but with a much purer test case, because we can perform the MD simulation with the GB Hamiltonian.

Therefore, for each of the snapshots generated with TIP4PEw water molecules, we performed either short MD simulations or steepest decent minimisations for 1, 3, 5, 10, 20, 50, 100, 200, or 1000 steps with a GBSA model and then evaluated the free energy in the normal way. The results are collected in Table 6 and they are presented as the difference compared to the sc-MM/GBSA estimates with the same GB model in Table 1.

It can be seen that with short MD simulations, the estimates converge towards the sc-MM/GBSA results but only slowly. For GBn there is a mean absolute deviation (MAD) of 43 kJ mol^{-1} after 10 MD steps, which is reduced to 7 kJ mol^{-1} after 1000 steps. In the latter case, the difference is not statistically significant for three of the ligands, but mostly owing to the poor precision of the GBn estimates. The situation is similar for GB^{OBCI}, although the differences were smaller from the start. After 1000 MD steps, the difference is 4 kJ mol^{-1} and the difference is not statistically significant for three ligands. However, for all the other numbers of MD steps, the MAD is actually larger than for the starting point.

Using minimisation with the GBn model, the differences compared to sc-MM/GBSA decrease somewhat, but very slowly. After 1000 steps of minimisation, the MAD is still 54 kJ mol^{-1}. Likewise, with the GB^{OBCI} model, the deviations have only decreased by 1 kJ mol^{-1} after 1000 steps. Hence, it seems very hard to correct the ensemble using minimisation. The reason for this is probably that the ensembles obtained by MD simulations and minimisations are different, which call into question the re-emerging suggestion to base MM/GBSA and similar approaches on minimised structures, rather than on MD snapshots (to save time).[34–37]

Structural differences in the binding site

A covariance analysis of the snapshots generated by TIP4PEw and GB^{OBCI} for each ligand shows that the structural differences in the binding site are similar for the various ligands. In summary, the binding site is slightly extended in the GB simulations, with the distance between the Trp-181 and Ser-237 backbones increasing by $\sim$1 Å (Fig. 2 shows residues at the ligand-binding site). The interactions with the ligand also become slightly weaker, *e.g.* the distance from the Trp-181 sidechain is increased by $\sim$0.5 Å. This is also reflected in the calculated binding affinities, which are on average $\sim$8 kJ mol^{-1} less attractive when the GB^{OBCI} snapshots are employed (if both sets are evaluated with the same method, GB^{OBCI}).

The largest differences are seen for the conformation of Arg-144. In both available crystal structures (for ligands **2** and **3**),[12,13] the guanidine group of this residue forms a stacking interaction with

Table 6 Difference between sc-MM/GBSA estimates in Table 1 and MM/GBSA estimates obtained after short MD simulations or minimisations of the snapshots from the explicit simulation

Solvent	GBn							GB^{OBCI}						
# Steps	**2**	**3**	**4**	**5**	**6**	MAD	MAX	**2**	**3**	**4**	**5**	**6**	MAD	MAX
Molecular dynamics														
0	−93.0	−115.7	−49.0	−44.6	−57.9	72.0	115.7	−11.4	2.5	16.2	12.2	19.8	12.4	19.8
1	−91.8	−115.5	−49.2	−44.4	−57.4	71.7	115.5	−9.6	3.5	16.4	13.0	20.6	12.6	20.6
3	−83.7	−103.5	−38.4	−32.9	−47.7	61.2	103.5	−5.1	10.0	23.0	19.0	26.5	16.7	26.5
5	−76.4	−94.0	−30.4	−24.8	−39.6	53.0	94.0	−1.6	14.9	27.1	23.1	31.1	19.5	31.1
10	−68.2	−82.2	−21.8	−13.8	−29.9	43.2	82.2	−0.1	15.1	28.3	26.2	32.2	20.4	32.2
20	−49.2	−60.4	−24.0	−12.7	−27.3	34.7	60.4	6.9	19.8	29.3	29.3	35.1	24.1	35.1
50	−27.2	−20.6	19.2	24.6	10.4	20.4	27.2	8.2	20.1	30.6	30.4	36.7	25.2	36.7
100	−43.7	−14.7	60.9	59.0	54.5	46.6	60.9	−1.5	13.5	28.9	33.0	38.2	23.0	38.2
200	−2.2	21.7	20.2	16.0	14.0	14.8	21.7	−1.8	10.6	24.1	18.0	32.8	17.5	32.8
1000	3.0	−16.9	−2.6	−13.5	0.6	7.3	16.9	−6.6	8.5	1.2	1.3	0.5	3.6	8.5
Minimisation														
0	−93.0	−115.7	−49.0	51.5	−57.9	73.4	115.7	−11.4	2.5	16.2	12.2	19.8	12.4	19.8
1	−92.2	−115.3	−49.2	−45.2	−58.3	72.0	115.3	−10.8	2.4	16.1	12.0	19.2	12.1	19.2
3	−91.9	−115.3	−48.8	−44.7	−57.9	71.7	115.3	−10.6	2.9	16.5	12.0	19.2	12.2	19.2
5	−91.6	−114.8	−48.2	−44.4	−57.6	71.3	114.8	−10.4	3.4	16.4	12.1	20.3	12.5	20.3
10	−90.6	−113.0	−46.8	−42.3	−56.3	69.8	113.0	−9.6	4.3	17.9	13.9	22.2	13.6	22.2
20	−93.6	−115.4	−47.9	−43.7	−56.7	71.4	115.4	−8.2	5.9	18.9	14.5	21.7	13.9	21.7
50	−90.8	−101.8	−39.0	−33.3	−46.3	62.2	101.8	−10.0	3.9	17.7	16.1	21.7	13.9	21.7
100	−90.6	−100.4	−38.0	−32.6	−45.6	61.4	100.4	−10.4	3.4	17.1	16.0	22.1	13.8	22.1
200	−89.5	−99.3	−36.7	−30.1	−43.0	59.7	99.3	−10.9	3.2	17.1	16.3	22.2	13.9	22.2
1000	−92.1	−90.6	−31.2	−22.9	−35.0	54.3	92.1	−18.5	−2.3	10.1	10.0	17.2	11.6	18.5

MAD and MAX are the mean and maximum absolute differences for the five ligands.

the aromatic ring of the ligand, but with opposite faces of the ring in the two structures (the ring is also tilted by ~90 degrees; *cf.* Fig. 2). For ligands **2**, **5**, and **6**, the starting conformation (*i.e.* the crystal structure for **2**, **3**, and **3**, respectively) is kept in the TIP4PEw simulations, suggesting that the stacking interaction is stable in explicit water. In the GB^{OBCI} simulations, the Arg-144 appears much more flexible and occupies several conformations. Interestingly, in the GB^{OBCI} simulation of ligand **2**, the most populated conformation is the one corresponding to the crystal structure of ligand **3**. This suggests that the two conformations have similar stability and that the discrimination between them is sensitive to the force field, solvent model, and simulation methodology. For ligands **5** and **6**, the dominant conformation of Arg-144 in the GB^{OBCI} simulation does not interact with the ligand at all, which leads to a decrease in van der Waals attraction by ~20 kJ mol^{-1} (see Table 3B). For ligands **3** and **4**, the stacking interaction is lost already in the TIP4PEw simulations in favour of an interaction with the side of the ring. Nevertheless, the interaction becomes even weaker when using the GB^{OBCI} model. These results are summarized in Fig. 3, which shows the distribution of the distance between the Arg-144 guanidine group and the aromatic ring of the ligand for various simulations.

The corresponding results for two time-points from the short GB^{OBCI} MD simulations are also shown in Fig. 3. It is evident that after 200 steps, the predominant conformation of Arg-144 is still the same as in the TIP4PEw simulations. On the other hand, after 1000 steps, the conformational distribution has started to shift towards the equilibrated GB^{OBCI} distribution for three of the ligands (and in the opposite direction for one ligand). Similar trends are seen for the binding site as a whole. For the three "well-behaving" ligands, **2**, **5**, and **6**, the RMSD of the binding site (the ligand and the ten closest residues) relative to the average GB^{OBCI} structure decreases slightly during the short GB^{OBCI} simulations; the ensemble initiated with TIP4PEw snapshots relaxes towards the fully equilibrated GB^{OBCI} ensemble, as expected, although 1000 steps is too short to see a full convergence. On the other hand, for ligands **3** and **4**, the RMSD relative to the average GB^{OBCI} structure actually increases during the short simulations, suggesting the presence of many accessible conformations. However, the low deviation (only 1.2 kJ mol^{-1}) between the binding affinities calculated using the 1000-step snapshots and the equilibrated GB^{OBCI} snapshots for ligand **4** (see Table 6) indicates that once the Arg-144 residue has lost its interaction with the ligand, its exact position is not so important energetically.

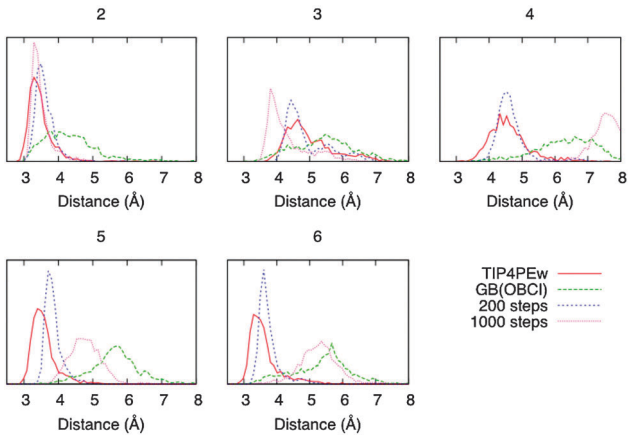

Fig. 3 Distribution of the minimum distance between the guanidine group of Arg-144 and the carbon atoms in the aromatic ring of the ligand over the 1600 snapshots from the TIP4PEw and GB^{OBCI} simulations, as well as from the short GB^{OBCI} MD simulations (200 or 1000 steps) initiated from the TIP4PEw snapshots. Results for all five ligands are shown.

It is also interesting to note that, for all ligands, a cluster analysis[38] performed on the coordinates of the ligand and the 10 closest residues places all the 1600 TIP4PEw snapshots in the same cluster, which means that there exists a snapshot which is within 1 Å RMSD of all the other snapshots. On the other hand, the same cluster analysis for the GB^{OBCI} snapshots gives 4–9 clusters (average 6.4) for the various ligands, showing that much more conformations of the binding site (in particular Arg-144) are sampled in the GB^{OBCI} simulations.

Conclusions

In this study we have computed MM/GBSA estimates of ligand-binding affinities using snapshots generated with MD simulations based on one explicit and two implicit-solvent models. We have compared the estimated affinities, and quantified the difference between the three snapshot ensembles. The study has provided several interesting results.

First, it is clear that the choice of solvent model both in the MD and in the energy calculations strongly affects the accuracy and precision of the estimates, as shown in Tables 1 and 2. For this test case, it is best to both run the MD simulations and to post-process the snapshots using the GB^{OBCI} model, although MD simulations with GBn followed by energy calculations with GB^{OBCI} give similar results. However, this is most certainly not a general conclusion, considering the small test set used and the fact that the explicit-solvent simulations gave structures closest to the crystal structure. Similar large differences between MM/GBSA energies obtained with the GBn and GB^{OBCI} have also been observed previously for the avidin protein.[9] In both studies, it was clear that GBn exaggerated the range of the binding affinities, leading to a relatively large MUEtr, although the ranking of the ligands can be as good or better than those obtained with GB^{OBCI}. The best approach would be to evaluate the free energies by free-energy perturbation methods and explicit water. However, if one chooses to use an implicit model in the evaluation of free energy, as in the MM/GBSA approach, it is no longer certain that structures generated with explicit water molecules will give better results than those generated with implicit water, even if the former are closer to the crystal structure. In our case, the results actually become worse, which may be related to the inconsistency of not reweighting the snapshots.

Second, it is very hard to distinguish the generated ensembles by a simple RMSD analysis. It is clear that both GB models show more variability among the snapshots than TIP4PEw, and that GBn shows less variation than GB^{OBCI}. Furthermore, we have

shown that the inter-ensemble variability is larger than the intra-ensemble variability, *i.e.*, the snapshots from distinct ensembles are more different than snapshots from the same ensemble. However, it is not possible to show by the RMSD analysis which ensemble is most different. In the binding site, the most prominent differences caused by the solvation model are seen for Arg-144, which adopts a much greater variety of conformations in the GB simulations than in the explicit-solvent simulations.

Third, we have attempted to convert the explicit-solvent snapshots to solvent-consistent snapshots by performing short MD simulations or minimisations with a GBSA model on the snapshots before evaluating the MM/GBSA free energy. Using MD, the results converge slowly towards sc-MM/GBSA estimates, although more than 1000 steps or 2 ps of simulation seem to be required before the results converge. This is a significant amount of time (3.2 ns for all 1600 snapshots) compared to the total 13 ns used for the MD simulations of standard (and sc-) MM/GBSA. Using minimisations instead of simulations, seems to show even worse convergence. Most likely the explicit-solvent and the implicit-solvent snapshots represent two distinct energy minima that are not easily interconvertible. The results indicate that MM/GBSA based on minimisations does not give the same results as standard MM/GBSA based on MD simulations.

Most importantly, the present results show that the standard MM/GB(PB)SA approach is inconsistent in that it uses snapshots sampled with explicit water molecules, but then calculates energies on these snapshots with an implicit-solvent model without reweighting the snapshots. Our result shows that such an approach gives results that are very different from the consistent approach of using the same solvent model in both the simulations and energy calculations. However, we do not expect that the sc-MM/GBSA approach will be significantly more accurate than standard MM/GBSA, because both approaches are limited by other approximations inherent in the method.[9,10,39]

Recently, there has been quite some interest in performing MM/GBSA-like calculations in which energies are calculated with quantum-mechanical (QM) methods.[40,41] Then, a similar question arises whether the MD snapshots obtained with MM methods are representative also of energy calculations with QM. Experience from reaction energies indicates that MM and QM potentials are so different that MM → QM reweighting normally does not converge, unless the QM system is kept fixed.[42–44] In this paper, we have instead tried to obtain the correct ensemble with short MD simulations or minimisations. Unfortunately, it seems that a large number of MD steps are needed for convergence (>1000), which would be prohibitive for most QM applications.

Acknowledgements

This investigation has been supported by grants from the Swedish research council (project 2010-5025) and from the Research School in Pharmaceutical Science at Lund University. It has also been supported by computer resources of Lunarc at Lund University.

References

1 J. Srinivasan, T. E. Cheatham III, P. Cieplak, P. A. Kollman and D. A. Case, *J. Am. Chem. Soc.*, 1998, **120**, 9401–9409.
2 P. A. Kollman, I. Massova, C. Reyes, B. Kuhn, S. Huo, L. Chong, M. Lee, T. Lee, Y. Duan, W. Wang, O. Donini, P. Cieplak, J. Srinivasan, D. A. Case and T. E. Cheatham, III, *Acc. Chem. Res.*, 2000, **33**, 889–897.
3 N. Foloppe and R. Hubbard, *Curr. Med. Chem.*, 2006, **13**, 3583–3608.
4 N. Homeyer and H. Gohlke, *Mol. Inf.*, 2012, **31**, 114–122.
5 I. Massova and P. A. Kollman, *J. Am. Chem. Soc.*, 1999, **121**, 8133–8143.
6 V. Zoete and O. Michielin, *Proteins: Struct., Funct., Bioinf.*, 2007, **67**, 1026–1047.
7 M. R. Lee, J. Tsai, D. Baker and P. A. Kollman, *J. Mol. Biol.*, 2001, **313**, 417–430.
8 B. R. Miller III, T. D. McGee Jr., J. M. Swails, N. Homeyer, H. Gohlke and A. E. Roitberg, *J. Chem. Theory Comput.*, 2012, **8**, 3314–3321.
9 S. Genheden, T. Luchko, S. Gusarov, A. Kovalenko and U. Ryde, *J. Phys. Chem. B*, 2010, **114**, 8505–8516.
10 A. Weis, K. Katebzadeh, P. Söderhjelm, I. Nilsson and U. Ryde, *J. Med. Chem.*, 2006, **49**, 6596–6606.
11 S. Genheden and U. Ryde, *J. Comput. Chem.*, 2010, **31**, 837–846.
12 P. Sörme, P. Arnoux, B. Kahl-Knutsson, H. Leffler, J. M. Rini and U. J. Nilsson, *J. Am. Chem. Soc.*, 2005, **127**, 1737–1743.
13 C. Diehl, O. Engström, T. Delaine, M. Håkansson, S. Genheden, K. Modig, H. Leffler, U. Ryde, U. Nilsson and M. Akke, *J. Am. Chem. Soc.*, 2010, **132**, 14577–14589.
14 V. Hornak, R. Abel, A. Okur, B. Strockbine, A. Roitberg and C. Simmerling, *Proteins: Struct., Funct., Bioinf.*, 2006, **65**, 712.
15 J. M. Wang, R. M. Wolf, K. W. Caldwell, P. A. Kollman and D. A. Case, *J. Comput. Chem.*, 2004, **25**, 1157–1174.
16 C. I. Bayly, P. Cieplak, W. D. Cornell and P. A. Kollman, *J. Phys. Chem.*, 1993, **97**, 10269–10280.
17 B. H. Besler, K. M. Merz and P. A. Kollman, *J. Comput. Chem.*, 1990, **11**, 431–439.
18 J. Mongan, C. Simmerling, J. A. McCammon, D. A. Case and A. Onufriev, *J. Chem. Theory Comput.*, 2007, **3**, 156–169.
19 A. Onufriev, D. Bashford and D. A. Case, *Proteins*, 2004, **55**, 383–394.
20 A. Bondi, *J. Phys. Chem.*, 1964, **68**, 441–451.
21 B. Kuhn and P. A. Kollman, *J. Med. Chem.*, 2000, **43**, 3786–3791.
22 J. Weiser, P. S. Shenkin and W. C. Still, *J. Comput. Chem.*, 1999, **20**, 217–230.
23 X. Wu and B. R. Brooks, *Phys. Lett.*, 2003, **381**, 512–518.
24 J. P. Ryckaert, G. Ciccotti and H. J. C. Berendsen, *J. Comput. Phys.*, 1977, **23**, 327–341.
25 H. W. Horn, W. C. Swope, J. W. Pitera, J. D. Madura, T. J. Dick, G. Hura and T. Head-Gordon, *J. Chem. Phys.*, 2004, **120**, 9665–9678.
26 H. J. C. Berendsen, J. P. M. Postma, E. F. van Gunsteren, A. DiNola and J. R. Haak, *J. Chem. Phys.*, 1984, **81**, 3684–3690.

27 M. R. Shirts, D. L. Mobley, J. D. Chodera and V. S. Pande, *J. Phys. Chem. B*, 2007, **111**, 13052–13063.
28 T. Darden, D. York and L. Pedersen, *J. Chem. Phys.*, 1993, **98**, 10089–10092.
29 S. Genheden and U. Ryde, *Proteins*, 2012, **80**, 1326–1342.
30 J. Kongsted and U. Ryde, *J. Comput. Aided Mol. Des.*, 2009, **23**, 63–71.
31 S. Genheden, O. Kuhn, P. Mikulskis, D. Hoffmann and U. Ryde, *J. Chem. Inf. Model.*, 2012, **52**, 2079–2088.
32 M. Kolar, J. Fanfrik and P. Hobza, *J. Phys. Chem. B*, 2011, **115**, 4718–4724.
33 V. M. Anisimov and C. N. Cavasotto, *J. Comput. Chem.*, 2011, **32**, 2254–2263.
34 B. Kuhn, P. Gerber, T. Schultz-Gasch and M. Stahl, *J. Med. Chem.*, 2005, **48**, 4040–4048.
35 G. Rastelli, A. Del Rio, G. Degliesposti and M. Sgobba, *J. Comput. Chem.*, 2010, **31**, 797–810.
36 C. R. W. Guimaraes and M. Cardozo, *J. Chem. Inf. Model.*, 2008, **58**, 958–970.
37 C. Rapp, C. Kalyanaraman, A. Schiffmiller, E. L. Schoenbrun and M. P. Jacobson, *J. Chem. Inf. Model.*, 2011, **51**, 2082–2089.
38 X. Daura, K. Gademann, B. Jaun, D. Seebach, W. F. Van Gunsteren and A. E. Mark, *Angew. Chem., Int. Ed.*, 1999, **38**, 236–240.
39 S. Genheden, P. Mikulskis, L. Hu, J. Kongsted, P. Söderhjelm and U. Ryde, *J. Am. Chem. Soc.*, 2011, **133**, 13081–13092.
40 K. Raha, M. B Peters, B. Wang, N. Yu, A. M. Wollacott, L. M. Westerhoff and K. M. Merz, *Drug Discovery Today*, 2007, **12**, 725–731.
41 P. Söderhjelm, S. Genheden and U. Ryde, *Quantum mechanics in structure-based ligand design*, in *Protein–ligand interactions*, ed. H. Gohlke, Methods and principles in medicinal chemistry, Wiley-VCH Verlag, Weinheim, 2012, vol. 53, pp. 121–143.
42 R. P. Muller and A. Warshel, *J. Phys. Chem. B*, 1995, **99**(17), 516.
43 T. H. Rod and U. Ryde, *Phys. Rev. Lett.*, 2005, **94**, 138302.
44 J. Heimdal and U. Ryde, *Phys. Chem. Chem. Phys.*, 2012, **14**, 12592–12604.